OXFORD

Human Molecular Genetics, 2023, Vol. 32, 5, 764–772
https://doi.org/10.1093/hmg/ddac229
Advance access publication date 20 September 2022
Original Article

A novel recessive mutation in *OXR1* is identified in patient with hearing loss recapitulated by the knockdown zebrafish

Yuan Li[1,†], Guozhu Ning[2,3,†], Baoling Kang[4], Jinwen Zhu[4], Xiao-Yang Wang[5], Qiang Wang[2,*] and Tao Cai[6,7,*]

[1]Department of Otorhinolaryngology, China-Japan Friendship Hospital, Beijing 1000292, China
[2]Division of Cell, Developmental and Integrative Biology, School of Medicine, South China University of Technology, Guangzhou 5100063, China
[3]State Key Laboratory of Membrane Biology, Institute of Zoology, University of Chinese Academy of Sciences, Chinese Academy of Sciences, Beijing 1001014, China
[4]Bioinformatics Section, Angen Gene Medicine Technology, Beijing 1001765, China
[5]VitroVivo Biotech LLC, Rockville, MD 208506, USA
[6]Experimental Medicine Section, National Institute of Dental and Craniofacial Research, NIH, Bethesda, MD 208927, USA
[7]Laboratory of Molecular Biology, National Institute of Diabetes and Digestive and Kidney Diseases, NIH, Bethesda, MD 20892, USA

*To whom correspondence should be addressed: Email: (Qiang Wang) qiangwang@scut.edu.cn; (Tao Cai) tcai@mail.nih.gov
†Co-first authors.

Abstract

Hereditary hearing loss is a highly genetically heterogeneous disorder. More than 150 genes have been identified to link to human non-syndromic hearing impairment. To identify genetic mutations and underlying molecular mechanisms in affected individuals and families with congenital hearing loss, we recruited a cohort of 389 affected individuals in 354 families for whole-exome sequencing analysis. In this study, we report a novel homozygous missense variant (c.233A > G, p.Lys78Arg) in the *OXR1* gene, which was identified in a 4-year-old girl with sensorineural hearing loss. *OXR1* encodes Oxidation Resistance 1 and is evolutionarily conserved from zebrafish to human. We found that the ortholog *oxr1b* gene is expressed in the statoacoustic ganglion (SAG, a sensory ganglion of ear) and posterior lateral line ganglion (pLL) in zebrafish. Knockdown of *oxr1b* in zebrafish resulted in a significant developmental defect of SAG and pLL. This phenotype can be rescued by co-injection of wild-type human *OXR1* mRNAs, but not mutant *OXR1* (c.233A > G) mRNAs. OXR1-associated pathway analysis revealed that mutations of *TBC1D24*, a TLDc-domain-containing homolog gene of OXR1, have previously been identified in patients with hearing loss. Interestingly, mutations or knockout of OXR1 interacting molecules such as ATP6V1B1 and ESR1 are also associated with hearing loss in patients or animal models, hinting an important role of *OXR1* and associated partners in cochlear development and hearing function.

Introduction

Hearing loss is the most common form of sensory disorder in humans, affecting 360 million persons worldwide. Nearly one in 1000 newborns has congenital hearing impairment, and >50% congenital hearing loss is attributable to heredity. More than 150 genes have been found to cause hearing impairment (1–3). Approximately 30–40% of hereditary deafness are syndromic and 60–70% are non-syndromic (4). More than 400 syndromes have been identified that include hearing loss. Several syndromes with hearing loss, such as Pendred syndrome (OMIM: 274600), Waardenburg syndromes (OMIM: 131244; OMIM: 193510, etc.), BOR syndrome (OMIM: 113650) and Usher syndromes (OMIM: 276900; OMIM: 605472, etc.), are often reported (5).

Next-generation sequencing (NGS) technologies have been widely used for identification of causative DNA variants in various Mendelian disorders. Specific gene mutations in patients with hearing loss could to be identified by genomic sequencing analyses (6). Mutations in the *POU3F4* gene were first discovered in 1995 as a cause of non-syndrome hearing loss (NSHL) (7). Mutations in *GJB2* and *GJB3*, which are a common cause of NSHL in many populations, were subsequently identified (8,9).

In a national survey of disabled persons in China, 27.8 million people were found to have hearing and speech disability (10). Nearly 30 000 babies are born with congenital sensorineural hearing loss (SNHL) each year (11,12). Previously, studies have shown that variations in *GJB2*, *SLC26A4*, *mtDNA* and *GJB3* are the most common variants associated with NSHL in the Chinese population (13). However, the mutation spectrums of congenital hearing loss are broad and diverse in Chinese. Most mutations are extremely rare and are only detected in a single or a few families (14).

We recently recruited a cohort of 389 individuals in 354 families with congenital hearing loss for whole-exome sequencing (WES) analysis. Here, we report the identification of a novel missense variant (c.233A > G, p.Lys78Arg) in the *OXR1* gene in a child with congenital NSHL by quad-WES analyses. We generated an animal model to investigate the role of the orthologue gene of *OXR1* in auditory organ development of zebrafish.

Result

Clinical description of the affected individual

The proband is the second child of non-consanguineous healthy Chinese parents (Fig. 1A). She was born by caesarean section at

Received: April 28, 2022. **Revised:** August 23, 2022. **Accepted:** September 3, 2022
Published by Oxford University Press 2022.

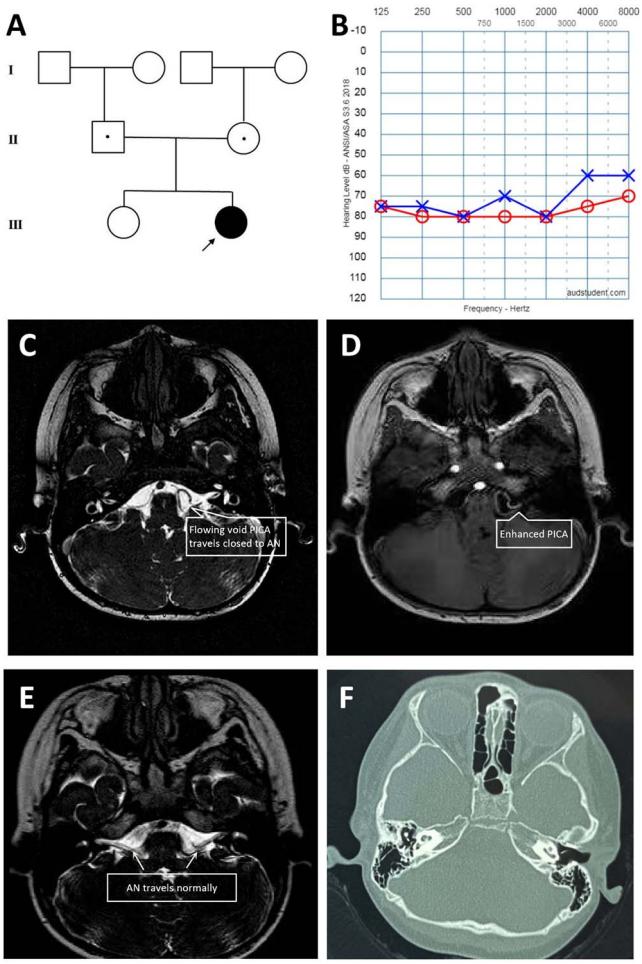

Figure 1. (**A**) Three-generation family pedigree for the affected individual. (**B**) Pure tone audiometry shows bilateral severe SNHL. ABR is absent under maximum stimuli. (**C–E**) Cranial MRI (axial) shows normal inner ear structure and a variant PICA. AN, auditory nerve. (**F**) HRCT of temporal bone shows normal bony inner ear structure.

term (38^{+4} W) after an uneventful pregnancy. Her birth weight was 3000 g and body length 50 cm. She failed to pass neonatal hearing screening. Audiological examinations, including visual reinforcement audiometry, auditory brainstem responses (ABRs), multifrequency steady-state response (ASSR) and distortion product otoacoustic emission (DPOAE) at 6 months, 1 year and 2 years of age, indicated that she had bilateral severe SNHL (Fig. 1B). Brain magnetic resonance imaging (MRI) (Fig. 1C–E) revealed that the left posterior inferior cerebellar artery (PICA) was tortuous, which was considered as an anatomic variation. High-Resolution Computed Tomography (HRCT) scan did not find pathological changes of her temporal bone (Fig. 1F).

The affected girl started to use a hearing aid for both ears at 2-year-old. She had mild speech delay and spoke in short sentences. Her intellectual ability and behavioral evaluation were normal. She also had a good athletic ability. No hearing loss history was found in other family members. In physical examination, her occipital frontal head circumference and her height were within normal ranges. EEG and other neurological examinations were also normal.

Identification of a novel homozygous missense mutation in OXR1

Parents-children quad-WES analysis for all the family members identified a previously undescribed homozygous missense mutation (c.233A > G, p.Lys78Arg, Fig. 2A) of the *OXR1* gene (GenBank acc. no., NM_001198533) in the 4-year-old girl with hearing loss. Her parents and her elder sister were all heterozygous carriers of this allele. This variant was extremely rare ($f = 0.000184$, homozygous = 0 in gnomAD database). To check the frequency of this allele in local population, 50 unrelated DNA samples were examined by Sanger sequencing with the primers specific for the c.233A-containing region. However, no c.233A > G or other variants were identified from these samples, confirming c.233A > G in the *OXR* gene is a rare variant.

Multiple-sequence alignment showed that the Lys78 is evolutionarily conserved in all vertebrates from zebrafish to human (Fig. 2B). Potential pathogenetic effect of this variant was predicted to be likely pathogenic by several commonly used tools, including Polyphen-2_HVAR, MutationTaster, VEST3, CADD (Supplementary Material, Table S1). However, several other tools like SIFT, Provean and Varsome predicted to be tolerable or uncertain significance (Supplementary Material, Table S1). Therefore, it is likely that the heterozygote carriers like the proband's parents are phenotypically normal, whereas the homozygote carrier like the proband could be affected.

According to UniProtKB and SmartMotif, the encoded OXR1 protein contains three domains (Fig. 2A): LysM (p.99–p.142), GRAM (p.208–p.275) and TLDc (p.713–p.874). Human Genomic Mutation Database (HGMD) listed two previously reported OXR1 variants: the heterozygous p.W5* variant was identified from three siblings with language impairment and the *de novo* heterozygous p.S192* from an individual with atrioventricular canal defects. Of note, four bi-allelic LoF variants (p.S367*, p.S442Vfs*2, c.2082 + 1G > T and c.2236-1G > C) in OXR1 were previously identified, but not yet collected by HGMD, in five affected individuals with neurological diseases, such as intellectual disability, developmental delay, cerebellar atrophy and seizures (Fig. 2A) (15). The three-dimensional protein structure of OXR1 is first modeled to predict the effect of the missense mutation on the protein using AlphaFold 2 protein structure database (https://alphafold.ebi.ac.uk/). More detailed analysis using SPDBV program reveals a new hydrogen bond is generated between the mutated residue R78 and Q77, which is not seen in the wild-type residue K78 (Fig. 2C).

Expression studies of *OXR1* ortholog genes in zebrafish

Previous studies showed that *oxr1a* and *oxr1b* expression are enriched in the central nervous system in zebrafish (16,17). To assess the role of *OXR1* in auditory system, we first investigated the expression patterns of *oxr1a* and *oxr1b* during zebrafish embryo development. Whole-mount *in situ* hybridization (WISH) was carried out using antisense RNA probes. As shown in Figure 3A, maternal *oxr1b* transcript was detected at the one-cell stage, but the zygotic expression of *oxr1b* was not observed before or during the tailbud stage. At the 10-somite stage, *oxr1b* transcript was present in the prechordal plate. Interestingly, *oxr1b* was specifically expressed in the olfactory bulbs and the tissues adjacent to anterior and posterior otic vesicle at 24 and 36 hpf (Fig. 3B and C). In addition, *oxr1b* was mainly expressed in the central nervous system during later stages (Fig. 3B). In contrast, there was no detectable expression of *oxr1a* in statoacoustic ganglion (SAG) or posterior lateral line ganglion (pLL). Instead, *oxr1a* was mainly expressed in the central nervous system (Supplementary Material, Fig. S1), which is consistent with previous report (18). These results indicate that *oxr1b* is possibly expressed in the SAGs and pLLs around the developing inner ear. To further confirm this, two-color fluorescent hybridizations were performed in the *Tg(HuC:GFP)*

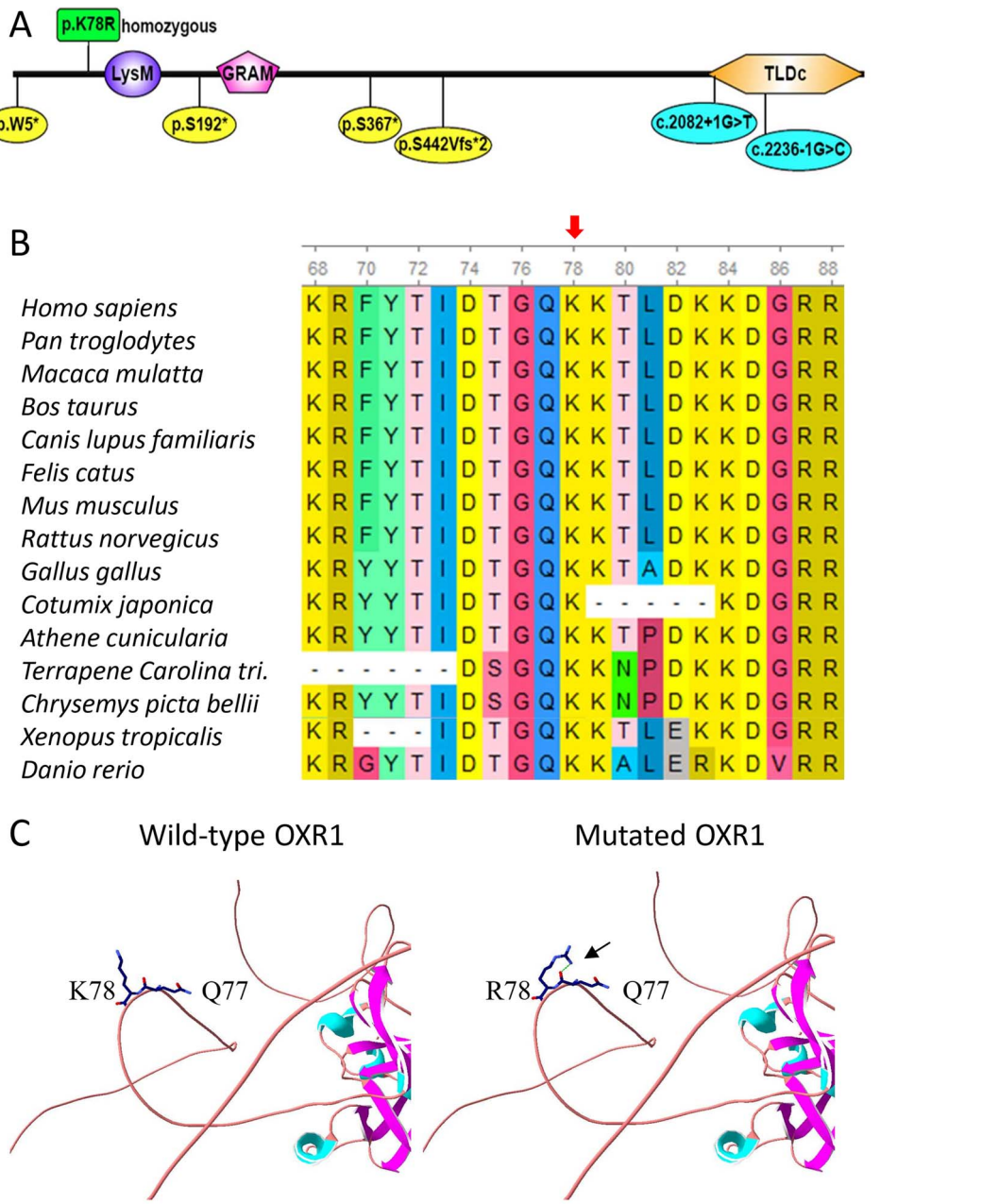

Figure 2. Mutation analysis of OXR1. (**A**) The current c.233A > G, p.Lys78Arg mutation as indicated by a green box and all reported six different LoF mutations of OXR1 are mapped to the schematic OXR1 protein. (**B**) Multiple sequence alignment of 16 different species using ClustalW program. The p.Lys78 residue as indicated by a red arrow is evolutionarily conserved from zebrafish to human. (**C**) Three-dimensional protein structure analysis using SPDBV program for protein active site interactions reveals a new hydrogen bond (indicated by a dotted green line) is generated between the mutated residue R78 and Q77 (right), which is not seen in the wild-type residue K78 (left).

embryos, where the SAGs and pLLs were labeled with GFP. Clearly, *oxr1b* transcripts (in red) were colocalized with the GFP signals in SAGs and pLLs at 24 and 36 hpf (Fig. 3D).

Knockdown of *oxr1b* expression impairs SAG development

To investigate the effect of *oxr1b* expression on SAG and pLL development, we applied antisense morpholino oligonucleotides (*oxr1b* MO) to block the splicing of *oxr1b* RNA at the junction of exon3/intron3 (Fig. 4A). After injection of 4 ng *oxr1b* MO, endogenous *oxr1b* mRNA expression was significantly reduced; the interfered mRNA product was obviously elevated (Fig. 4B). Meanwhile, these morphants showed a normal appearance compared with the control embryos at 24 hpf (Fig. 4C). Notably, the expression of *oxr1b* in SAG and pLL was almost totally abolished in the morphants (Fig. 4D). These results indicate a high efficiency of *oxr1b* MO in blocking the expression of *oxr1b*. We next examined the expression levels of *neurod1* and *neurogenin1*, two widely used markers for SAG and pLL development (19), in wild-type embryos and *oxr1b* morphants at 24 hpf. Obviously, *oxr1b* inactivation was found to lead to a reduction of *neurogenin1* expression in both SAG and pLL (Fig. 5A). On the other hand, the expression of *neurod1* was clearly declined in SAG, but not in pLL (Fig. 5A). These observations suggest that *oxr1b* may play a primary role in

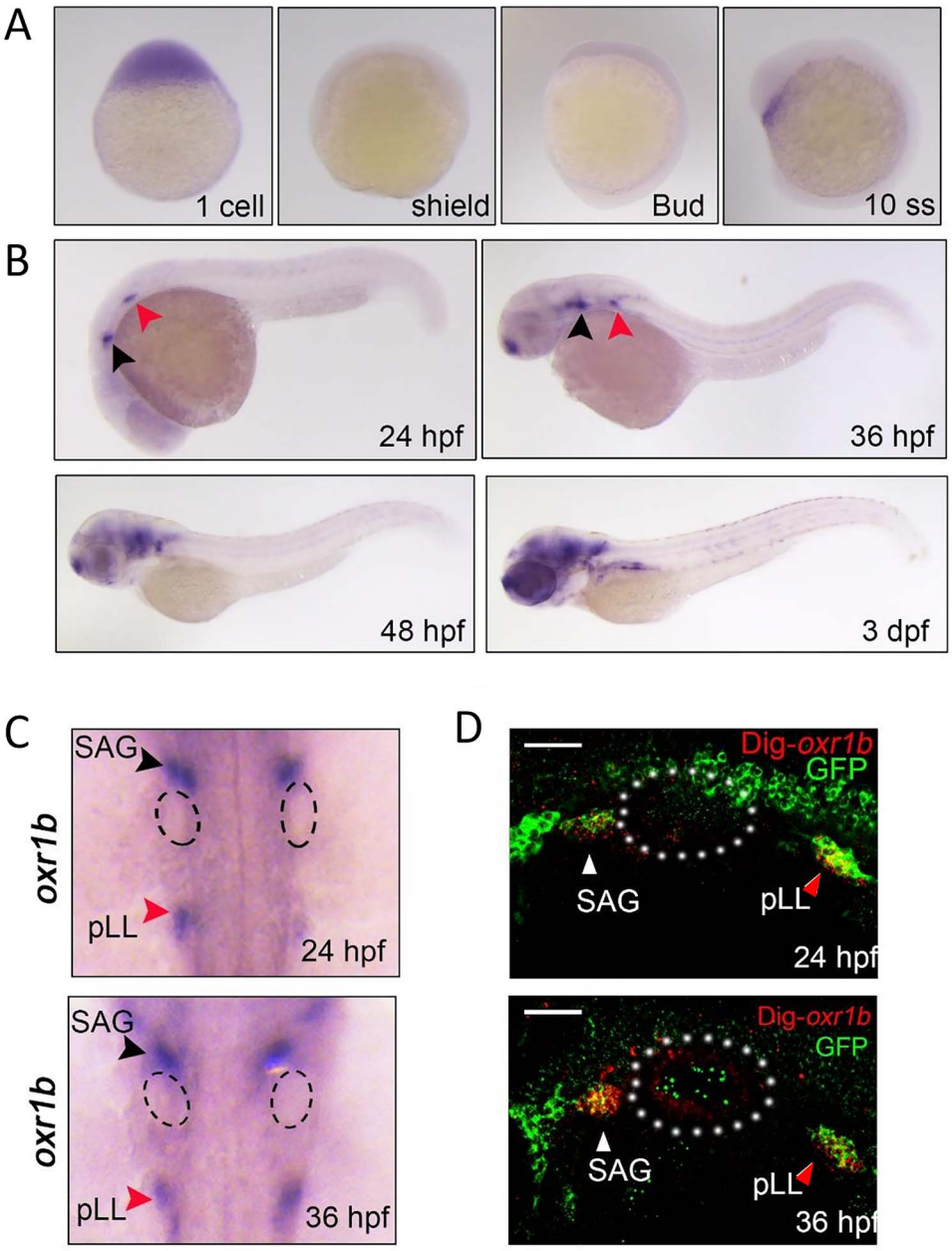

Figure 3. Expression of *oxr1b* in the SAG and pLL. (**A**) Analysis of *oxr1b* expression at different stages by *in situ* hybridization. (**B**) Lateral views (anterior to the left. Scale bar, 50 μm) of *oxr1b* expression in SAG as indicated by black arrow heads and pLL indicated by red arrow heads at 24, 36, 48 hpf and 3 dpf. (**C**) Dorsal views of *oxr1b* expression at 24 and 36 hpf. Black and red arrow heads indicate SAG and pLL, respectively. Black dotted lines indicate otic vesicles. (**D**) Spatiotemporal analysis of *oxr1b* expression in *Tg (HuC:GFP)* embryos. At 24 and 36 hpf, *Tg(HuC:GFP)* transgenic embryos are stained with *oxr1b* probe (red), and then immunostained with anti-GFP antibody (green). The SAG and pLL are indicated by white and red arrowheads, respectively. The otic vesicles are indicated by white dotted circles. SAG, statoacoustic ganglion; pLL, posterior lateral line ganglion.

SAG development. In supporting this finding, knocking down of *oxr1b* expression in the *Tg(HuC:GFP)* transgenic embryos indeed impaired the formation of SAG but not pLL (Fig. 5B). Therefore, *oxr1b* is indeed required for SAG development.

K78R-containing OXR1 could not rescue SAG formation defect

To confirm whether the c.233A > G;p.K78R mutation could affect the function of *OXR1* in SAG development, human wide-type or mutant *OXR1* mRNAs were co-injected with MO into one-cell stage embryos. Overexpression of the wide-type *OXR1* clearly rescued the developmental defects of SAG (Fig. 6). However, co-injection of the mRNAs encoding *OXR1* K78R mutant failed to relieve the defects in SAG formation (Fig. 6A). Thus, these results imply the K78R mutation in OXR1 may contribute substantially to the SAG development in zebrafish, hinting its pathogenic effects in SNHL in the patient.

To assess whether the hearing is impaired in *oxr1b* morphants or not, we examined the fast escape reflex. We first injected 4 ng or 5 ng of *oxr1b*-MO into wild-type embryos, which did not impair the zebrafish hearing. Low dosage of *oxr1b*-MO may not be sufficient to knockdown its function because the SAGs development may be recovered during later embryo development stages. However, when 6 ng of *oxr1b*-MO was injected, 5/6

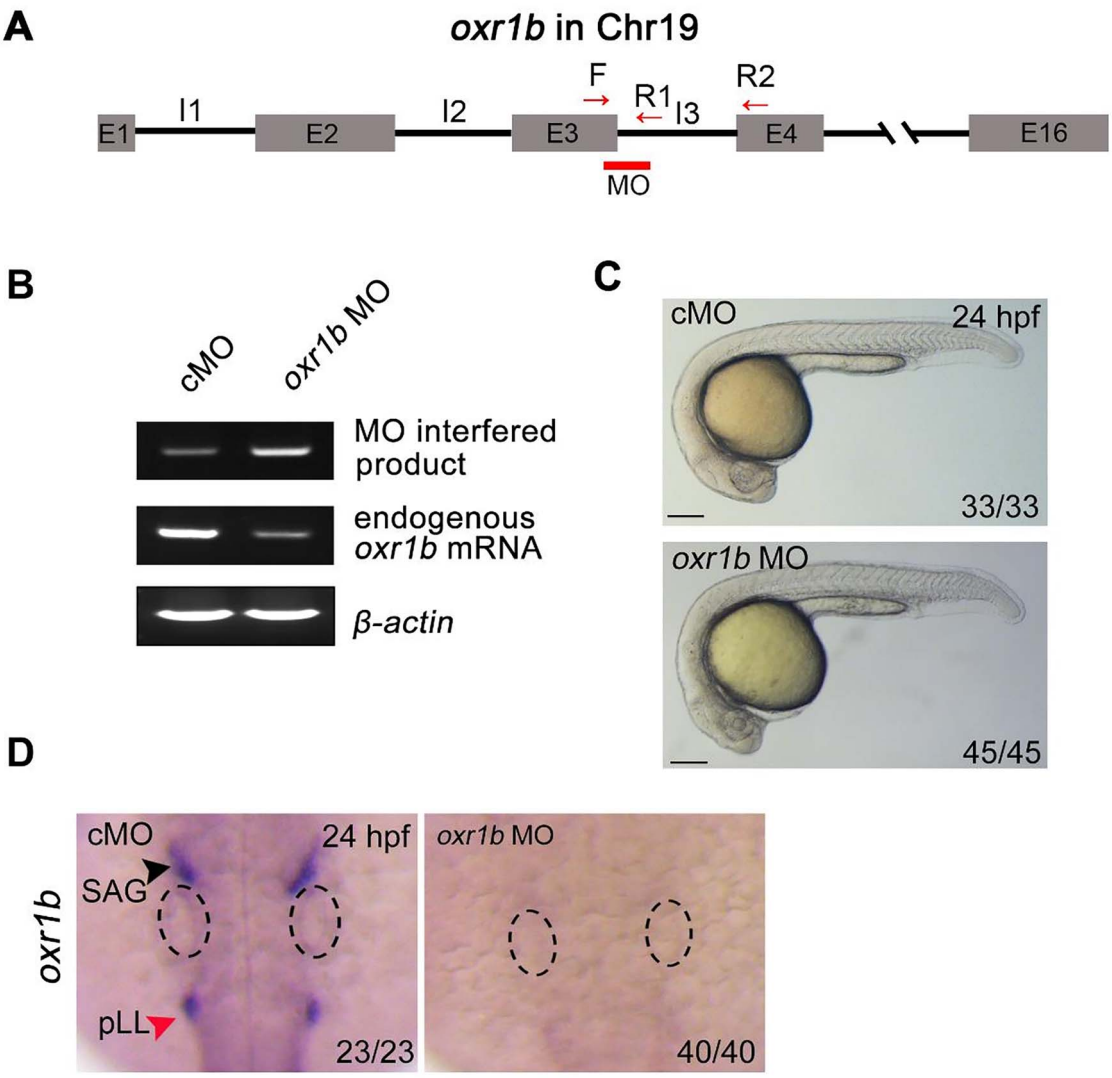

Figure 4. Knockdown of *oxr1b* expression using splice-blocking MO in zebrafish. (**A**) Schematic genomic structure of the *oxr1b* gene in chromosome 19. The MO targeting site (in red bar) is between exon 3 (E3) and intron 3 (I3). Locations of PCR primers are indicated by red arrows. (**B**) Evaluation of effectiveness of the *oxr1b* MO. Note that the MO interfered *oxr1b* mRNA is increased in the morphants, whereas endogenous mRNA is significantly deceased. *β*-actin is served as a control. (**C**) Morphological effects of wild-type embryos injected with 4 ng cMO or *oxr1b* MO. Scale bar, 200 μm. (**D**) Expression of *oxr1b* in wild-type embryos injected with 4 ng cMO or *oxr1b* MO. Embryos are injected with indicated MO at the one-cell stage, and then harvested at 24 hpf for *in situ* hybridization. The ratio of affected embryos is indicated. Note that *oxr1b* expression is disrupted in the morphants.

wild-type embryos became no response to external sound stimulation. The velocity (mm/s) of their movements was close to 0. Only 1/6 of zebrafish larvae showed a weak motor ability after sound stimulation (Supplementary Material, Fig. S2).

Discussion

OXR1, also known as *TLDC3*, belongs to a conserved family of genes related to the reactive oxygen species (ROS) in eukaryotic species (20). *OXR1* encodes Oxidation Resistance Protein 1, which is predicted to enable oxidoreductase activity and to protect cells and organisms against oxidative stress (21). OXR1 has been found to be a therapeutic target for several neurodegenerative diseases, such as Parkinson's disease, hyperoxia induced retinopathy and neuronal damage (22). Previous studies identified multiple bi-allelic loss-of-function mutations in *OXR1* from five individuals with autosomal recessive cerebellar atrophy and lysosomal dysfunction (15). However, no hearing loss was reported in these affected individuals with brain developmental disorders or epilepsy. Our case on the other hand may reveal a specific effect of the extremely rare missense mutation (c.233A > G, p.Lys78Arg) on hearing function.

Knockout *Oxr1* in mice was found to cause apoptosis in the granule cell (GC) layer of the cerebellum because of oxidative stress conditions (23). In zebrafish, *oxr1a* and *oxr1b* (two orthologues of *Oxr1*), were found to express in central nervous system (18). Zebrafish *oxr1a* $^{-/-}$ displays a short life-span, premature ovarian failure and increased expression levels of early stress response genes, such as *gpx1b, gpx4a, gpx7* and *sod3a* (16). Zebrafish *oxr1b* $^{-/-}$ was previously shown to cause down-regulation of multiple antioxidant genes, thereby resulting in hypersensitive to oxidative stress (17).

Cochlea is an important auditory organ (24,25). Many qualitative studies have shown that hearing loss is because of cochlear

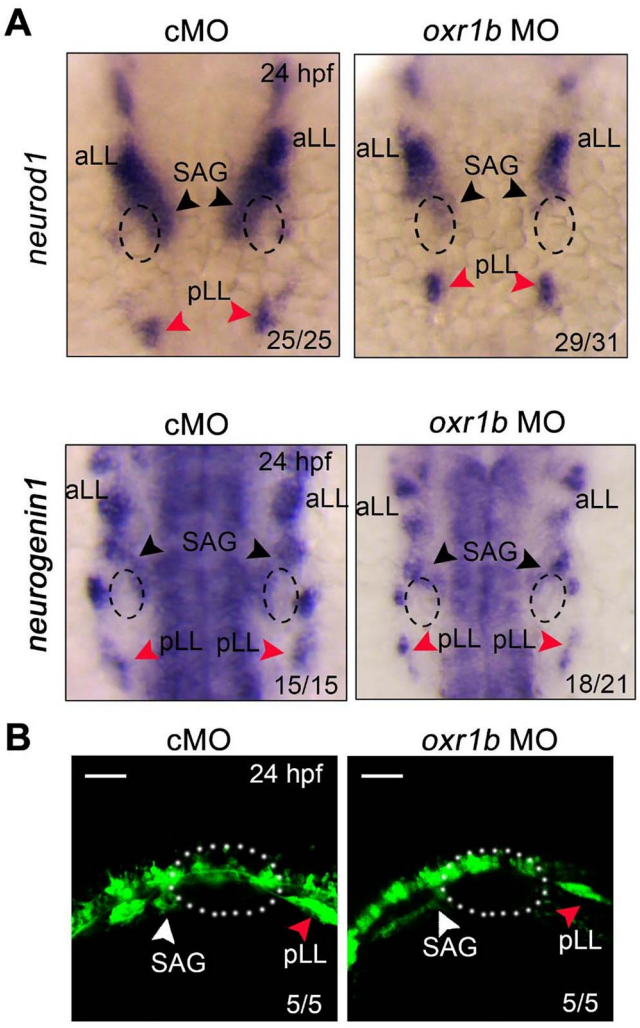

Figure 5. *oxr1b* is required for SAG development. (**A**) The expression patterns of SAG markers (*Neurod1* and *Neurogenin1*) embryos injected with 4 ng cMO or *oxr1b* MO. Embryos are injected with indicated MO at the one-cell stage, and then subjected to WISH at 24 hpf. Dorsal views with anterior to the top. SAG and pLL are indicated by black and red arrowheads, respectively. (**B**) Representative confocal images of *Tg(HuC:GFP)* embryos injected with 4 ng cMO or *oxr1b* MO. SAG and pLL are indicated by white and red arrowheads, respectively. Otic vesicles are indicated by white dotted circles. SAG, statoacoustic ganglion. pLL, posterior lateral line ganglion. Lateral views, anterior to the left. Scale bar, 50 μm.

hair cell damage (26). The neurons of SAG are the key to receive and emit sensory information through the hair cells (27). In zebrafish, *neurogenin1* and *neurod1* have been demonstrated to play important roles in the development of otic placode and cranial ganglia, such as SAG, anterior lateral line ganglia and posterior lateral line ganglia (28–30). However, how other genes that contribute to statoacoustic neurons development and associated hearing function are not fully understood.

In this study, we show for the first time that *oxr1b* (an ortholog of human *OXR1*) is highly expressed in SAG in zebrafish and plays a pivotal role in SAG neuron formation. To model the OXR1-associated hearing loss because of the c.233A > G (p.K78R) variant in *OXR1*, we knocked down *oxr1b* expression using antisense splicing morpholino in zebrafish and found development defects of SAG tissue in morphants. Moreover, rescue experiments via co-injection of human wild-type *OXR1* mRNA largely rescued the MO-induced phenotypes,whereas the c.233A > G mutant *OXR1* mRNA could not rescue the SAG defect. The *oxr1b* morpholino-treated zebrafish embryos failed to show obvious response to the C-startle stimulation, whereas the wide-type control larvae did. However, *oxr1b* may also play a role in central nervous system in late embryonic development because of its abundant expression in the CNS region (Fig. 3B). Future studies, given a stable mutant could be established by CRISPR/Cas9 genome editing technology, can explore the underlying molecular mechanisms of *OXR1* in the hearing-associated pathway.

OXR1 protein contains three conserved domains: LysM, GRAM and TLDc, the latter is known to be a core domain indispensable to antioxidant defenses (15,21,31), which interacts with H_2O_2 via oxidation of a reactive cysteine (Cys753) in TLDc (23). OXR1 is localized in cytoplasm and controls mitochondrial resistance to oxidative stress via regulating antioxidant pathways involving the p21 molecule (32,33). In addition, our preliminary data showed the stabilities of the OXR1 protein were not affected by the p.K78R mutation (Supplementary Material, Fig. S3). However, whether or not the p.K78R mutant affects antioxidant process remains to be elucidated.

Previous studies showed that OXR1 and its homologues NCOA7 are associated with the V-ATPases (34). However, no evidence was shown that NCOA7 is also expressed in cochlear. Therefore, further analysis of OXR1 protein interactome in cochlear-associated tissues may reveal OXR1-associated molecular-genetic mechanisms underlying hearing loss. For instance, TBC1D24 is a homolog of OXR1 in the family of TLDc-domain-containing genes (21). At least 27 different mutations (21 missense and 6 LoF variants) in *TBC1D24* have been identified in affected individuals with hearing loss (35–37). Notably, >70 different variants in *OXR1* have been linked to epilepsy, intellectual disability and other developmental defects (HGMD). On the basis of String database (https://string-db.org/, Version 11.5) (38), OXR1 is linked to 10 predicted functional partners (Supplementary Material, Fig. S4). Interestingly, the hearing-loss-causal gene ATP6V1B1 was predicted to interact with OXR1 and also confirmed by experiment analyses (34). As we know, at least 26 different variants of *ATP6V1B1* have been identified in patients with hearing loss (HGMD).

In addition, protein–protein interacting analysis in mouse revealed that OXR1 also interacts with ESR1 (Supplementary Material, Fig. S5), which was confirmed by associated experiments (39). It is known that both Esr1 and Esr2 are present in some neurons of the inner ear, suggesting their specific functions in hearing (39). Specially, *Esr2* knockout mice showed absence of hear cells and became deaf at 1 year of age, suggesting estrogen has a direct effect on the hearing function (39). At human level, mutations in *ESR1* have been linked to multiple disorders, including autosomal recessive estrogen resistance (OMIM: 615363) and autosomal dominant migraine (OMIM: 157300). Mutations in *ESR2* were also linked to autosomal dominant Ovarian dysgenesis 8 (OMIM: 618187). Therefore, both *ESR1* and *ESR2* could be good candidate genes for affected individuals with hearing loss.

Taken together, we identified a homozygous missense mutation in the novel candidate gene *OXR1* in a patient with hearing-loss. Functional studies demonstrated that knockdown of *oxr1b* expression in zebrafish dramatically affects SAG development. Furthermore, human wild-type *OXR1* mRNA, but not the p.K78R missense mutation-containing mRNA, could rescue the oxr1b-knockdown-associated SAG development defects. As a novel candidate gene, additional mutations in *OXR1* should be screened from larger populations with hearing loss.

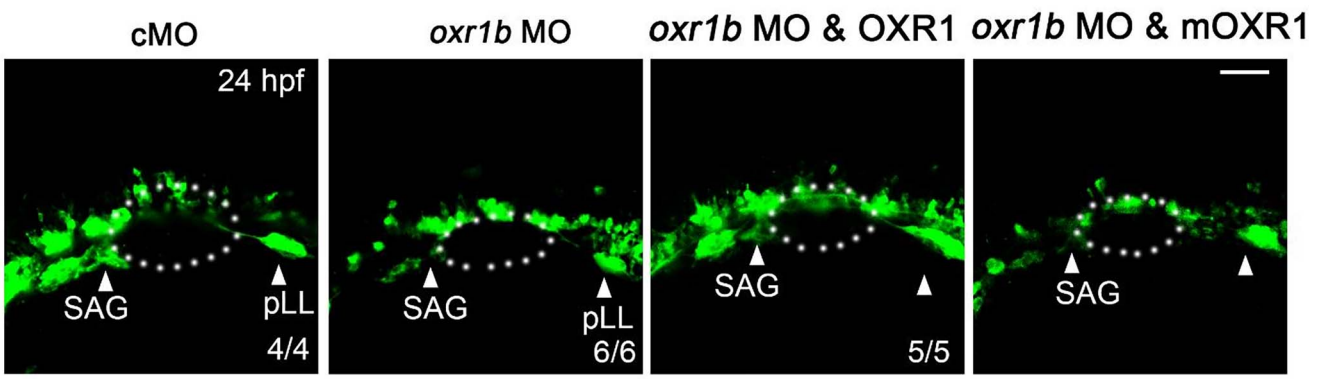

Figure 6. *oxr1b* inactivation-induced SAG defect is rescued by overexpression of wide-type human *OXR1* but *mutated OXR1* (*mOXR1*, c.233A > G). *Tg(HuC:GFP)* embryos were injected with indicated MO and mRNA at the one-cell stage, and then harvested at 24 hpf for live-imaging. The otic vesicles are indicated by white dotted circles. SAG, statoacoustic ganglion; pLL, posterior lateral line ganglion. Injection dose: cMO, 4 ng; *oxr1b* MO, 4 ng; *OXR1* mRNA, 50 pg; *mOXR1* mRNA, 50 pg. Scale bar, 50 μm.

Materials and Methods

Clinical evaluation

A cohort of 389 affected individuals in 354 families with congenital hearing loss were recruited for WES analysis. Neonatal hearing screenings were examined using automated otoacoustic emissions measurements (Interacoustics otoread-screener, Szczecin, Polska, Poland). Detailed medical histories were collected for all affected individuals and their families, including basic information, gestation and birth history, drug use during pregnancy and their family histories. Investigations were carried out on the basis of the patients' clinic symptoms and histories. General physical examination, mental and behavioral tests, audiology and speech tests, radiological investigations, such as high-resolution CT and MRI scans, were performed for each of the affected individuals.

WES and bioinformatics analysis

Genomic DNAs were extracted from peripheral blood cells of the participants. Whole-exomes were captured by SureSelect Human All Exon kit (Agilent), followed by high-throughput sequencing by HiSeq2000 sequencer (Illumina Inc.). Genomic reads were aligned for SNP calling and further analysis for identification of deleterious variants which are predicted by multiple commonly used programs, such as MutationTaster, Polyphen-2 and SIFT. Detected variants with minor allele frequency (MAF) > 0.001 on the basis of gnomAD or in-house Chinese Exome Database were eliminated. Selected variants in candidate genes were further verified by Sanger sequencing with specific primers.

Zebrafish embryo preparation and startle response test

Wild-type (Tübingen) and *Tg(HuC:GFP)* zebrafish lines were maintained under standard laboratory conditions. All live zebrafish embryos were raised at 28.5°C in Holtfreter's solution and staged by morphology as previously described (40). All zebrafish experiments were approved and carried out in accordance with the Animal Care Committee at the Institute of Zoology, Chinese Academy of Sciences (Permission number IOZ-13048). Sound-evoked C-shaped startle response for zebrafish with or without hearing loss, as previously described (41), was examined at 5 dpf in a well-plate and recorded using a camera. Pure tone stimulations (600 Hz, 80 dB) were administered.

Whole mount *in situ* hybridization

Total RNAs were extracted by using TRIzol reagent (15596018, Invitrogen) at 24 h post fertilization (hpf), and reverse-transcribed into cDNA using ReverTra ace kit (Toyobo, Osaka, Japan). The produced total cDNAs were used to amplify required segments of *oxr1a* (ENSDART00000159249.2) and *oxr1b* (ENSDART00000151137.3) transcripts by two pair of primers: 1) *oxr1a*, forward 5′-AGGAATCACTCATGCAAAACCTTCG-3′; reverse 5′-CGAAGAAGAGCTCTGTATTAAATGC-3′; 2) *oxr1b*, forward 5′-AAACTTTCAGACCCAATCTCACCGA-3′ and reverse 5′-CCACGTC CAGAAATGAAGTGCAAAT-3′. PCR products were purified and cloned into the pGMT vector (VT202–02, TIANGEN Company, China). Antisense RNA probes were transcribed *in vitro* using MEGAscript kit (Ambion) according to the manufacturer's instructions. Whole mount *in situ* hybridization and two-color fluorescent *in situ* hybridization were performed as described previously (42,43).

Morpholino and mRNAs injections

The standard negative control morpholino (cMO) was 5′-CCTCTTACCTCAGTTA CAATTTATA-3′. The *oxr1b* splice-blocking Morpholino (Gene Tools, USA) sequence was 5′-AGTAAACACCTA CTACTCACCACGT-3′. For rescue studies, the full length cDNAs of human *OXR1* (ENST00000442977.6) and mutant *OXR1* (c.233A > G: p.K78R) were amplified by RT-PCR (forward primer 5′-AGCGGATC CATGTCTGTGTCTAATCTATCATGGC-3′ and reverse primer 5′-AGGTCTAGATTATTCAAAAGCCCAGATTTCAATA-3′), and then cloned into the pCS2-HA vector. The plasmids were linearized with NotI restriction enzyme (NEB, R0189M) and mRNAs were synthesized *in vitro* using the mMessage mMachine T7 Transcription kit (Ambion, Austin, USA). Microinjection was performed as previously described (43).

Western blotting

HEK293T cells were transfected with the plasmids HA-OXR1 or HA- mOXR1. The transfected cells were subjected to Cycloheximide (CHX) treatment (5 μg/ml) for 2–6 h and then lysed by using TNE lysis buffer (10 mM Tris–HCl, pH 7.5, 150 mM NaCl, 2 mM EDTA and 0.5% Nonidet P-40) containing a protease inhibitor cocktail. Affinity-purified anti-HA (1:3000; CW0092A, CWBIO) and anti-β-actin (1:3000, CW0096, CWBIO) were used for immunoblotting. CHX was purchased from AMRESCO and dissolved in DMSO.

Living imaging

Tg(HuC:GFP) embryos were anaesthetized at 24 or 36 hpf and then embedded in 1% low-melt agarose. Confocal stack pictures of the otic vesicle-containing region were taken using a Nikon A1R+ confocal microscope (20× dry).

Supplementary Material

Supplementary Material is available at *HMG* online.

Acknowledgements

We are thankful for the affected individual and her family who participated in this study. We also want to thank Drs Dong Liu and Jie Gong (Nantong University, Nantong, China) for their help on the analysis of C-startle response.

Conflict of Interest statement. Baoling Kang and Jinwen Zhu were employed at Angen Gene Medicine Technology Company at Beijing at the time of submission. No other conflicts relevant to this study should be reported.

Funding

Audiology Development Foundation of China (NO53100000500 017757XA19013) to ANGEN Inc., Beijing. This study was also supported by the National Natural Science Foundation of China (32025014 and 31872838) and the National Key Research and Development Program of China 671 (2018YFA0800200 and 2020YFA0804000). The funders had no role in study design, data collection and analysis, decision to publish, or preparation of the manuscript.

Authors' contributions

Y.L. and T.C. conceived the study. T.C. wrote the final manuscript, with contributions from all co-authors. Y.L. collected clinic data; G.N. performed and analyzed zebrafish data, which was evaluated by Q.W.; B.K. and J.Z. analyzed WES data.

References

1. Cryns, K. and Van Camp, G. (2004) Deafness genes and their diagnostic applications. *Audiol. Neurootol.*, **9**, 2–22.
2. Petit, C., Levilliers, J. and Hardelin, J.P. (2001) Molecular genetics of hearing loss. *Annu. Rev. Genet.*, **35**, 589–645.
3. Raviv, D., Dror, A.A. and Avraham, K.B. (2010) Hearing loss: a common disorder caused by many rare alleles. *Ann. N. Y. Acad. Sci.*, **1214**, 168–179.
4. Tekin, M., Arnos, K.S. and Pandya, A. (2001) Advances in hereditary deafness. *Lancet*, **358**, 1082–1090.
5. Babanejad, M., Beheshtian, M., Jamshidi, F., Mohseni, M., Booth, K.T., Kahrizi, K. and Najmabadi, H. (2022) Genetic etiology of hearing loss in Iran. *Hum. Genet.*, **141**, 623–631.
6. Atik, T., Bademci, G., Diaz-Horta, O., Blanton, S.H. and Tekin, M. (2015) Whole-exome sequencing and its impact in hereditary hearing loss. *Genet Res (Camb)*, **97**, e4.
7. de Kok, Y.J., van der Maarel, S.M., Bitner-Glindzicz, M., Huber, I., Monaco, A.P., Malcolm, S., Pembrey, M.E., Ropers, H.H. and Cremers, F.P. (1995) Association between X-linked mixed deafness and mutations in the POU domain gene POU3F4. *Science*, **267**, 685–688.
8. Sloan-Heggen, C.M., Bierer, A.O., Shearer, A.E., Kolbe, D.L., Nishimura, C.J., Frees, K.L., Ephraim, S.S., Shibata, S.B., Booth, K.T., Campbell, C.A. *et al.* (2016) Comprehensive genetic testing in the clinical evaluation of 1119 patients with hearing loss. *Hum. Genet.*, **135**, 441–450.
9. Xia, J.H., Liu, C.Y., Tang, B.S., Pan, Q., Huang, L., Dai, H.P., Zhang, B.R., Xie, W., Hu, D.X., Zheng, D. *et al.* (1998) Mutations in the gene encoding gap junction protein beta-3 associated with autosomal dominant hearing impairment. *Nat. Genet.*, **20**, 370–373.
10. He, Z.H., Li, M., Zou, S.Y., Liao, F.L., Ding, Y.Y., Su, H.G., Wei, X.F., Wei, C.J., Mu, Y.R. and Kong, W.J. (2019) Protection and prevention of age-related hearing loss. *Adv. Exp. Med. Biol.*, **1130**, 59–71.
11. Dai, P., Liu, X., Yu, F. and Zhu, Q. (2006) Molecular etiology of patients with nonsyndromic hearing loss from deaf-mute schools in 18 provinces of China. *Chin J Otol*, **4**, 1–5.
12. Sun, X.B., Wei, Z.Y., Yu, L.M., Wang, Q. and Liang, W. (2008) Prevalence and etiology of people with hearing impairment in China. *Zhonghua Liu Xing Bing Xue Za Zhi*, **29**, 643–646.
13. Xuezhong, L.I.U. and O.X., Denise Yan. (2006) The genetic deafness in Chinese population. *J. Otol.*, **1**, 1–10.
14. Diaz-Horta, O., Duman, D., Foster, J., 2nd, Sirmaci, A., Gonzalez, M., Mahdieh, N., Fotouhi, N., Bonyadi, M., Cengiz, F.B., Menendez, I. *et al.* (2012) Whole-exome sequencing efficiently detects rare mutations in autosomal recessive nonsyndromic hearing loss. *PLoS One*, **7**, e50628.
15. Wang, J., Rousseau, J., Kim, E., Ehresmann, S., Cheng, Y.T., Duraine, L., Zuo, Z., Park, Y.J., Li-Kroeger, D., Bi, W. *et al.* (2019) Loss of oxidation resistance 1, OXR1, is associated with an autosomal-recessive neurological disease with cerebellar atrophy and lysosomal dysfunction. *Am. J. Hum. Genet.*, **105**, 1237–1253.
16. Xu, H., Jiang, Y., Li, S., Xie, L., Tao, Y.X. and Li, Y. (2020) Zebrafish Oxr1a knockout reveals its role in regulating antioxidant defenses and aging. *Genes (Basel)*, **11**, 1118–1141. https://doi.org/10.3390/genes11101118.
17. Xu, H., Wang, G., Chi, Y.Y., Kou, Y.X. and Li, Y. (2021) Expression profiling and functional characterization of the duplicated Oxr1b gene in zebrafish. *Comp. Biochem. Physiol. Part D Genomics Proteomics*, **39**, 100857.
18. Laroche, F.J., Tulotta, C., Lamers, G.E., Meijer, A.H., Yang, P., Verbeek, F.J., Blaise, M., Stougaard, J. and Spaink, H.P. (2013) The embryonic expression patterns of zebrafish genes encoding LysM-domains. *Gene Expr. Patterns*, **13**, 212–224.
19. Andermann, P., Ungos, J. and Raible, D.W. (2002) Neurogenin1 defines zebrafish cranial sensory ganglia precursors. *Dev. Biol.*, **251**, 45–58.
20. Volkert, M.R., Elliott, N.A. and Housman, D.E. (2000) Functional genomics reveals a family of eukaryotic oxidation protection genes. *Proc. Natl. Acad. Sci. U. S. A.*, **97**, 14530–14535.
21. Finelli, M.J. and Oliver, P.L. (2017) TLDc proteins: new players in the oxidative stress response and neurological disease. *Mamm. Genome*, **28**, 395–406.
22. Zorec, R., Parpura, V. and Verkhratsky, A. (2018) Preventing neurodegeneration by adrenergic astroglial excitation. *FEBS J.*, **285**, 3645–3656.
23. Oliver, P.L., Finelli, M.J., Edwards, B., Bitoun, E., Butts, D.L., Becker, E.B., Cheeseman, M.T., Davies, B. and Davies, K.E. (2011) Oxr1 is essential for protection against oxidative stress-induced neurodegeneration. *PLoS Genet.*, **7**, e1002338.
24. Delmaghani, S. and El-Amraoui, A. (2020) Inner ear gene therapies take off: current promises and future challenges. *J. Clin. Med.*, **9**, 2309–2336.
25. Lim, R. and Brichta, A.M. (2016) Anatomical and physiological development of the human inner ear. *Hear. Res.*, **338**, 9–21.
26. Zhong, C., Fu, Y., Pan, W., Yu, J. and Wang, J. (2019) Atoh1 and other related key regulators in the development of auditory sensory

epithelium in the mammalian inner ear: function and interplay. *Dev. Biol.*, **446**, 133–141.
27. Kelley, M.W. (2006) Regulation of cell fate in the sensory epithelia of the inner ear. *Nat. Rev. Neurosci.*, **7**, 837–849.
28. Kral, A., Kronenberger, W.G., Pisoni, D.B. and O'Donoghue, G.M. (2016) Neurocognitive factors in sensory restoration of early deafness: a connectome model. *Lancet Neurol.*, **15**, 610–621.
29. Taberner, L., Banon, A. and Alsina, B. (2018) Anatomical map of the cranial vasculature and sensory ganglia. *J. Anat.*, **232**, 431–439.
30. Vemaraju, S., Kantarci, H., Padanad, M.S. and Riley, B.B. (2012) A spatial and temporal gradient of Fgf differentially regulates distinct stages of neural development in the zebrafish inner ear. *PLoS Genet.*, **8**, e1003068.
31. Murphy, K.C. and Volkert, M.R. (2012) Structural/functional analysis of the human OXR1 protein: identification of exon 8 as the anti-oxidant encoding function. *BMC Mol. Biol.*, **13**, 26.
32. Elliott, N.A. and Volkert, M.R. (2004) Stress induction and mitochondrial localization of Oxr1 proteins in yeast and humans. *Mol. Cell. Biol.*, **24**, 3180–3187.
33. Yang, M., Luna, L., Sorbo, J.G., Alseth, I., Johansen, R.F., Backe, P.H., Danbolt, N.C., Eide, L. and Bjoras, M. (2014) Human OXR1 maintains mitochondrial DNA integrity and counteracts hydrogen peroxide-induced oxidative stress by regulating antioxidant pathways involving p21. *Free Radic. Biol. Med.*, **77**, 41–48.
34. Merkulova, M., Paunescu, T.G., Azroyan, A., Marshansky, V., Breton, S. and Brown, D. (2015) Mapping the H(+) (V)-ATPase interactome: identification of proteins involved in trafficking, folding, assembly and phosphorylation. *Sci. Rep.*, **5**, 14827.
35. Campeau, P.M., Kasperaviciute, D., Lu, J.T., Burrage, L.C., Kim, C., Hori, M., Powell, B.R., Stewart, F., Felix, T.M., van den Ende, J. *et al.* (2014) The genetic basis of DOORS syndrome: an exome-sequencing study. *Lancet Neurol.*, **13**, 44–58.
36. Rehman, A.U., Santos-Cortez, R.L., Morell, R.J., Drummond, M.C., Ito, T., Lee, K., Khan, A.A., Basra, M.A., Wasif, N., Ayub, M. *et al.* (2014) Mutations in TBC1D24, a gene associated with epilepsy, also cause nonsyndromic deafness DFNB86. *Am. J. Hum. Genet.*, **94**, 144–152.
37. Azaiez, H., Booth, K.T., Bu, F., Huygen, P., Shibata, S.B., Shearer, A.E., Kolbe, D., Meyer, N., Black-Ziegelbein, E.A. and Smith, R.J. (2014) TBC1D24 mutation causes autosomal-dominant nonsyndromic hearing loss. *Hum. Mutat.*, **35**, 819–823.
38. Szklarczyk, D., Gable, A.L., Nastou, K.C., Lyon, D., Kirsch, R., Pyysalo, S., Doncheva, N.T., Legeay, M., Fang, T., Bork, P., Jensen, L.J. and von Mering, C. (2021) The STRING database in 2021: customizable protein-protein networks, and functional characterization of user-uploaded gene/measurement sets. *Nucleic Acids Res.*, **49**, D605–D612.
39. Simonoska, R., Stenberg, A.E., Duan, M., Yakimchuk, K., Fridberger, A., Sahlin, L., Gustafsson, J.A. and Hultcrantz, M. (2009) Inner ear pathology and loss of hearing in estrogen receptor-beta deficient mice. *J. Endocrinol.*, **201**, 397–406.
40. Kimmel, C.B., Ballard, W.W., Kimmel, S.R., Ullmann, B. and Schilling, T.F. (1995) Stages of embryonic development of the zebrafish. *Dev. Dyn.*, **203**, 253–310.
41. Zhang, L., Gao, Y., Zhang, R., Sun, F., Cheng, C., Qian, F., Duan, X., Wei, G., Sun, C., Pang, X. *et al.* (2020) THOC1 deficiency leads to late-onset nonsyndromic hearing loss through p53-mediated hair cell apoptosis. *PLoS Genet.*, **16**, e1008953.
42. He, J., Mo, D., Chen, J. and Luo, L. (2020) Combined whole-mount fluorescence in situ hybridization and antibody staining in zebrafish embryos and larvae. *Nat. Protoc.*, **15**, 3361–3379.
43. Jia, S., Wu, D., Xing, C. and Meng, A. (2009) Smad2/3 activities are required for induction and patterning of the neuroectoderm in zebrafish. *Dev. Biol.*, **333**, 273–284.